Anisotropic Standing-Wave Formation on an Au(111)-(23×√3) Reconstructed Surface

D. Fujita,* K. Amemiya, T. Yakabe, and H. Nejoh
National Research Institute for Metals, 1-2-1 Sengen, Tsukuba 305, Japan

T. Sato and M. Iwatsuki
JEOL Ltd., 3-1-2 Musashino, Akishima, Tokyo 196, Japan
(Received 30 September 1996)

Significant effects of the long-range "herringbone" reconstruction on the formation of standing waves in the Fermi-level surface-state electron density were observed for the first time on an Au(111)-(23 × $\sqrt{3}$) reconstructed surface using a low-temperature scanning tunneling microscope at 30 K. Enhanced oscillation of the surface local density of states was observed, especially along the pairwise soliton walls, which suggests the possible existence of anisotropic wave propagation. [S0031-9007(97)03153-0]

PACS numbers: 68.35.Bs, 61.16.Ch

Close-packed surfaces of noble metals are well known to have two-dimensional (2D) nearly free electron surface states, whose energy bands were reported to show isotropic dispersions in the *sp* band gaps of the projected bulk states [1–5]. Recently, scanning tunneling microscopy (STM) has revealed that interference of incident and scattered 2D electron waves at potential barriers results in the spatial modulation of the local density of states (LDOS) of the surface-state electrons [6–9]. Among the observed (111) surfaces of the noble metals, the Au(111) surface is especially interesting to study further because of the following reasons. Gold is the only face-centered-cubic (fcc) metal whose (111) surface reconstructs. Moreover, the reconstruction of the Au(111) surface is not a conventional one, but is a complex system consisting of both short-range (23 × $\sqrt{3}$) and long-range structures, called the "*herringbone*" pattern [10,11]. This herringbone reconstruction offers strikingly ordered adsorption and nucleation sites on the surface [12–14]. In spite of the interesting properties of the herringbone structure, its potential effects on standing-wave formation of the surface-state electrons have not been studied yet. Here, we report the first observation of the effects of the large-scale reconstruction on the interference of the 2D electron waves on the Au(111) surface using a low-temperature STM.

Experimental data shown here were obtained at ~30 K in ultrahigh vacuum of 3×10^{-9} Pa. The Au(111) sample was made by vapor deposition of gold on a mica substrate at 800 K and subsequent heating up to 1000 K in vacuum. The surface was cleaned with Ar ion sputtering and annealing at ~1000 K. Using this method, atomically flat Au(111) surfaces were routinely obtained [13]. Electrochemically etched tungsten tips were used for the STM measurements. After the sample preparation, STM images of the Au(111) reconstructed surface was observed with atomic resolution at room temperature (RT). The tunneling bias V_t is defined as the voltage of the sample measured with respect to the tip.

Figure 1(a) shows a STM image of the Au(111) surface ($V_t = 30$ mV, tunneling current $I_t = 0.3$ nA), which exhibits mostly the topographic nature of the surface. The upper and lower terraces are separated by a monatomic step of 0.24 nm height that corresponds well to the monatomic height of 0.236 nm on the Au(111) plane [14]. The image shows several pairs of bright stripes on the terraces. According to the proposed models for the reconstructed Au(111)-(23 × $\sqrt{3}$) surface [15,16], 23 gold surface atoms are packed on 22 bulk lattice sites along the $\langle 1\bar{1}0 \rangle$ direction in a unit cell, resulting in uniaxial contraction of 4.4%. Consequently, the surface atoms are forced to occupy the three different atomic-stacking sites such as normal fcc type (*ABC* . . .), hexagonal-close-packed (hcp) type (*ABA* . . .), and incommensurate type (*bridge site*). The observed ridges called "*soliton walls*" (*s*) are interpreted as transition regions consisting of bridge-site atoms, which separate fcc (*f*) and hcp (*h*) regions. Formation of zigzag patterns is characteristic of the herringbone reconstruction, and is explained by the spontaneous formation of "*stress domains*" in order to reduce the uniaxial surface stress [17].

By approaching the bias voltage very close to zero ($V_t = -2$ mV), the constant-current STM image showed a dramatic change, as shown in Fig. 1(b), which is almost the same area as Fig. 1(a). Compared with Fig. 1(a), the observed striking difference is the emergence of long-range spatial oscillations with a decay length of up to ~50 nm. Especially in the upper terrace near the step, the ripples with a constant periodicity of ~1.8 nm were clearly observed, being aligned parallel to the monatomic step. The most probable reason for the oscillatory structure is interference of waves. The LDOS of surface states on Au(111) and their interaction with monatomic steps were investigated earlier with STM and theory by Davis *et al.* [18], followed by Avouris *et al.* [9]. Based on their reports, the standing wave in the LDOS $\rho(k_{\|}, x)$ caused by the interference of electron waves at a step edge can be expressed as

 0031-9007/97/78(20)/3904(4)$10.00

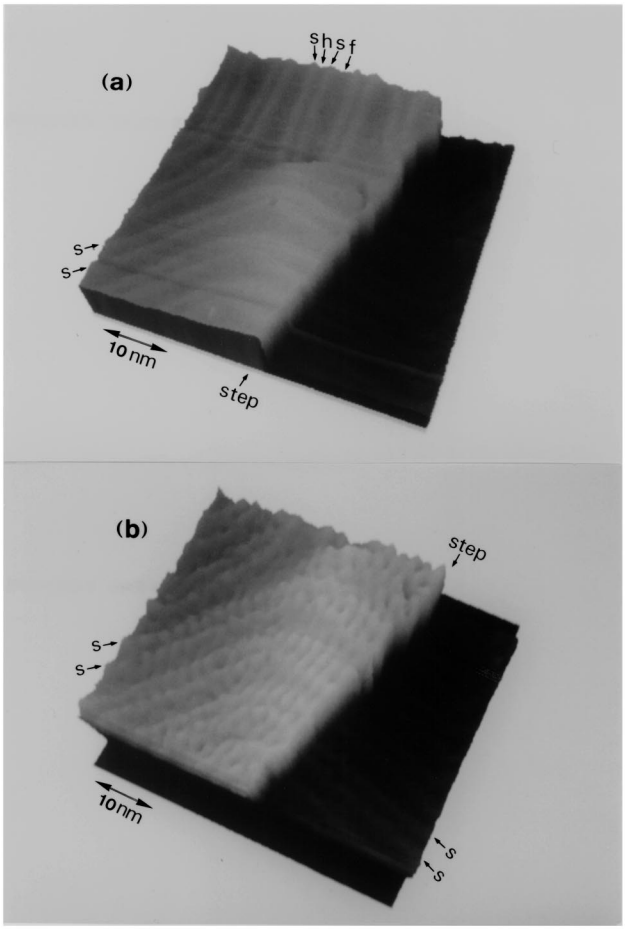

FIG. 1. (a) A constant-current image of the reconstructed Au(111) surface ($V_t = 30$ mV, $I_t = 0.3$ nA) at ~30 K. Two terraces are separated by a monatomic step of 0.24 nm height. Pairwise soliton walls (indicated as s) with a corrugation of ~0.015 nm are clearly evident, which are the transition regions between the hcp-like (h) and the fcc-like regions (f). (b) A constant-current image of almost the same area as above using an extremely low tunneling bias V_t of -2 mV ($I_t = 0.1$ nA). It is remarkable that long-range spatial oscillations have become distinct, especially near the step.

follows:

$$\rho(k_{\|}, x) = \rho_0\big(1 - J_0(2k_{\|}x)\big), \qquad (1)$$

where x is the distance from the step edge, $k_{\|}$ is the 2D wave number of surface-state electron, ρ_0 is the LDOS of the homogeneous free electron gas, and J_0 is the zeroth-order *Bessel* function. The observed oscillation has a characteristic periodicity L of 1.8 ± 0.1 nm, from which the wave number $k_{\|}$ can be deduced using the relation of $k_{\|} = \pi/L$. The estimated wave number $k_{\|}$ of ~1.7 nm^{-1} corresponds well to that of the previously reported wave number ($k_F = 1.73$ nm^{-1}) of the surface-state electrons at the Fermi level (E_F) [1]. Consequently, the origin of the oscillation can be attributed to the interference effect and the formation of standing waves in the surface-state electron density.

Although the image of Fig. 1(a) seemed to exhibit only the topography of the surface, differentiation and/or cross-sectional profiling made it possible to detect the faint oscillatory structures on the upper terrace near the step edge. The maximum corrugation was found to be only less than 0.005 nm, and the oscillation decayed more quickly within a few intervals. The reason why the standing waves were clearly observed in Fig. 1(b) can be explained as follows. By using an extremely low bias of -2 mV, the constant-current image corresponds directly to a Fermi-level LDOS contour of the surface-state electrons, taken at the center of the curvature of the tip [19]. If conventional voltages (~100 mV) are used, the image should be composed by summing all of the energy-resolved LDOS oscillations from E_F to the applied bias energy (eV). Superposition of waves with different periodicity must blur the structure of standing waves and reduce both the amplitude and the decay length.

A more astonishing observation is that the standing-wave oscillations were found to be strongly affected by the herringbone reconstruction structures. The observed amplitude of the LDOS oscillations was found to be inhomogeneous and dependent on the three regions with different geometries on the Au(111) reconstructed surface. Figure 2 shows cross-sectional profiles measured in the three regions near the step edge. In the hcp and the soliton-wall regions, the observed amplitudes of the standing waves are more enhanced than that in the fcc regions. The average corrugations caused by the standing-wave oscillations in the hcp and soliton-wall

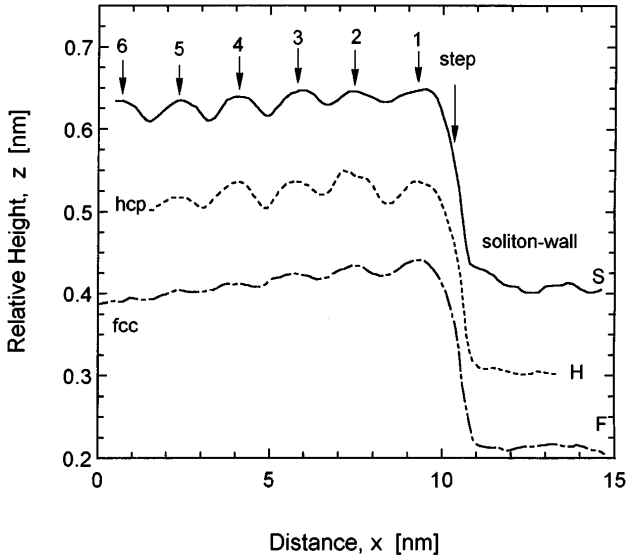

FIG. 2. Cross-sectional profiles of Fig. 1(b) measured perpendicular to the monolayer step along the soliton wall, the hcp, and the fcc regions. All profiles show oscillations of the surface LDOS with the same periodicity on the upper terrace. The corrugation caused by the standing-wave formation is more distinct in the case of the soliton-wall and the hcp region (~0.02 nm) than in the fcc case (~0.01 nm).

regions were about 0.02 nm, whereas that in the fcc regions was ~0.01 nm. Those differences in amplitudes may be attributed to the inhomogeneous distribution of the surface-state LDOS.

The reason why the herringbone effect can be observed distinctly at ~30 K can be attributed to the more enhanced elastic mean free path or coherence length of electrons at lower temperatures. Using the uncertainty relation for position and momentum, the coherence length λ_c can be expressed as

$$\lambda_c \cong 1/\Delta k_{\|}\,, \tag{2}$$

where $\Delta k_{\|}$ is a wave number spread of the 2D electrons at E_F. The energy dispersion relation for the free-electron-like surface-state electrons can be expressed as

$$E = \hbar^2 k_{\|}^2/2m^*, \tag{3}$$

where m^* is the effective mass of the surface-state electrons. Using the Fermi distribution function and the energy dispersion relation for the surface-state electrons, the wave number spread $\Delta k_{\|}$ can be expressed as follows:

$$\Delta k_{\|} = m^* \Delta E/\hbar^2 k_{\|}\,. \tag{4}$$

Thermal width ΔE can be evaluated as the full width at half maximum of the differential Fermi-distribution function, that is, $\sim 3.5 k_B T$, where k_B and T are Boltzmann's constant and temperature, respectively. Finally, the coherence length of the surface-state electrons can be expressed as below:

$$\lambda_c \cong \hbar^2 k_{\|}^2/3.5 m^* k_B T\,. \tag{5}$$

Using Eq. (5) and the reported values for m^* ($= 0.28 m_e$) and $k_{\|}$($= 1.73\ \mathrm{nm}^{-1}$) [1], the coherence length of surface-state electrons at E_F is estimated to be ~5 nm at 298 K. Since the coherence length at RT is much shorter than the typical width (~15 nm) of *stress domains* of the herringbone structure, it is reasonable that the previous studies at RT could not observe the effects of the herringbone reconstruction [7–9]. In contrast, at 30 K, the coherence length is evaluated as ~50 nm, which is almost consistent with the observed decay length for the standing waves. Since the coherence length at 30 K is much longer than the typical domain width (~15 nm), it is quite reasonable that the effects of long-range reconstruction has become observable at this temperature.

The other significant feature of the STM image at ~30 K is the observation of the enhanced standing-wave formation along the pairwise soliton walls. As shown in Fig. 3(a), the oscillation appear to be elongated along the pairwise soliton walls (*s*). Figure 3(b) shows cross-sectional profiles along a typical soliton wall. From the step edge to the first elbow positions along the soliton walls (*A*-*B*), the wave front is parallel to the step-edge line. At the first elbow positions (*e*), the soliton walls change their directions with an angle of about 60° to the left, because they enter another stress domain. In the second stress domain, along the soliton wall (*C*-*D*), we can still observe the oscillation with a similar periodicity L (1.9 ± 0.1 nm) and a slightly smaller corrugation ($0.01 \sim 0.02$ nm). If the direction of the standing waves from the step edge is unchanged, the interval of oscillation along the soliton walls in the second domain should be about twice ($= 1/\cos 60°$) as large as the initial periodicity L (~ 1.8 nm). However, the observed intervals along the soliton walls in the second domain are almost the same as the original periodicity observed near the step edge. That is, the electron waves appear to be propagating quasi-one-dimensionally along

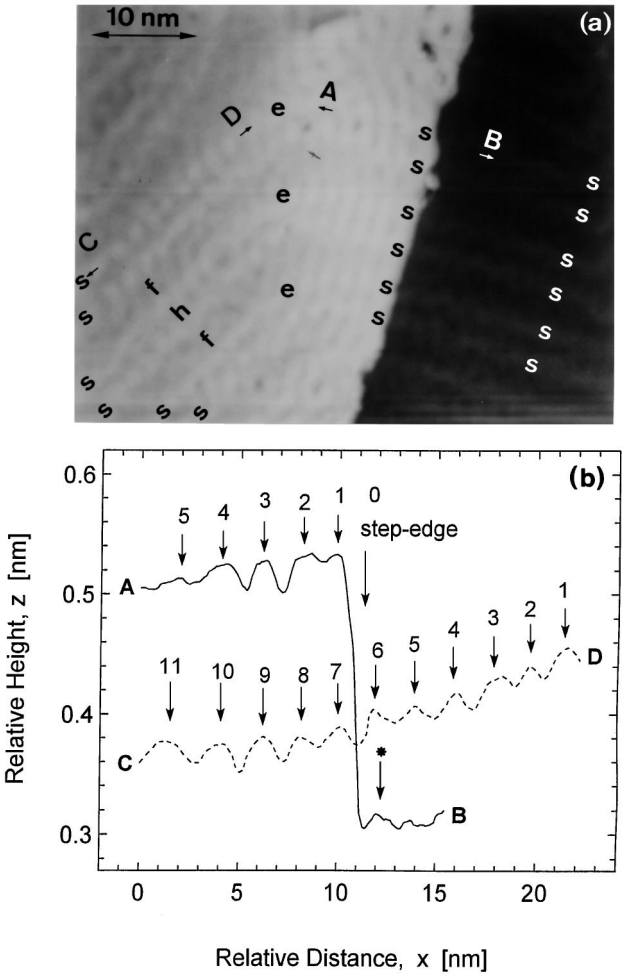

FIG. 3. (a) A constant-current 2D image of Au(111) observed at ~30 K ($V_t = -2$ mV, $I_t = 0.3$ nA). Amplitudes of the LDOS oscillation are different in the three regions, fcc (f), hcp (h), and soliton wall (s). It is observed that the direction of wave propagation along the soliton walls is apparently changed at the elbow positions (e). (b) Cross-sectional profiles between *A*-*B* and *C*-*D* lines along the same soliton wall, indicated in the above image. Arrows indicate the peak positions of the standing waves along the soliton wall. Both profiles shows oscillations of the surface LDOS with a similar interval ($L = 1.8$–1.9 nm). On the lower terrace, faint standing-wave formation was observed along the soliton wall as indicated the asterisk (*).

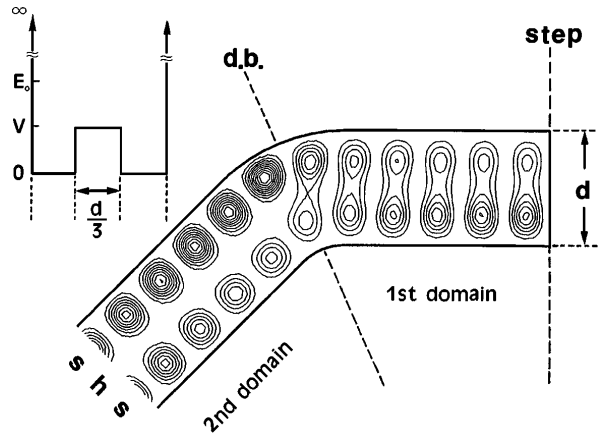

FIG. 4. Contours of the probability densities of the surface-state electrons of $k_{\|} = 3.2\pi/d$, which are confined in a quasi-one-dimensional waveguide with width d. The shape of potential walls is schematically based on the observed pairwise soliton walls (s) and the hcp region (h) from a step edge. One of the ends is terminated by an infinite potential barrier *(step)*. Change of direction occurs at the domain boundary ($d.b.$) between the stress domains.

the pairwise soliton walls. The probable explanations for the anisotropic standing-wave formation may be attributed to (1) the existence of the quasi-one-dimensional surface state along the pairwise soliton walls, or (2) the deflection of waves at the boundary between the adjacent stress domains. The former hypothesis seems probable since quantum confinement of originally extended surface states has been observed in other experiments such as a stepped surface of a Cu(100) [20] or H/Ni(110) system [21]. As for the latter model, which also seems possible, we should leave this question open for future work. In order to clarify the possibility of the first idea, we have developed a simple one-dimensional wave-guide model. As a first approximation, the surface-state electrons along the pairwise soliton walls are assumed to be confined to an infinitely long wave guide of width d. This wave guide is composed of one pair of soliton walls and one hcp region, whose potential is shown in the upper left of Fig. 4. The potential V in the hcp region is assumed to be half of the incident energy E_0. One of the ends is terminated by the potential barrier ("*step*"), and the other end is located infinitely far away. The probability density of electrons was calculated by solving the Schrödinger equation numerically using the so-called mode-matching method. The wave number $k_{\|}$ of the injected electrons is assumed to be $3.2\pi/d$, and the incident mode is the second mode. Although this model is a rough approximation, the calculated probability density shown in Fig. 4 can qualitatively reproduce the observed spatial modulation of the LDOS, which suggests the intrinsic anisotropy of surface-state electron behavior. In order to demonstrate this model, a detailed knowledge about the local potential distribution on the surface is required. Moreover, it can be inferred from this model that the local 2D Fermi surface might have some anisotropic nature.

In summary, we have observed the significant effects of the long-range reconstruction on the formation of standing waves in the surface LDOS on the Au(111) reconstructed surface at $\sim$30 K. The observed anisotropic standing waves suggest the important role of the herringbone structure on the interference of surface-state electrons, and the possible existence of one-dimension-like wave propagation along the pairwise soliton walls.

*Corresponding author.
Electronic address: fujitad@nrim.go.jp

[1] S. D. Kevan and R. H. Gaylord, Phys. Rev. B **36**, 5809 (1987).
[2] R. Paniago, R. Matzdorf, G. Meister, and A. Goldmann, Surf. Sci. **336**, 113 (1995).
[3] L. Hulbert, P. D. Johnson, N. G. Stoffel, W. A. Royer, and N. V. Smith, Phys. Rev. B **31**, 6815 (1985).
[4] L. Hulbert, P. D. Johnson, N. G. Stoffel, and N. V. Smith, Phys. Rev. B **32**, 3451 (1985).
[5] D. P. Woodruff, W. A. Royer, and N. V. Smith, Phys. Rev. B **34**, 764 (1986).
[6] M. F. Crommie, C. P. Lutz, and D. M. Eigler, Nature (London) **363**, 524 (1993).
[7] Y. Hasegawa and Ph. Avouris, Phys. Rev. Lett. **71**, 1071 (1993).
[8] Ph. Avouris and I.-W. Lyo, Science **264**, 942 (1994).
[9] Ph. Avouris, I.-W. Lyo, R. E. Walkup, and Y. Hasegawa, J. Vac. Sci. Technol. B **12**, 1447 (1994).
[10] Ch. Wöll, S. Chiang, R. J. Wilson, and P. H. Lippel, Phys. Rev. B **39**, 7988 (1989).
[11] J. V. Barth, H. Brune, G. Ertl, and R. J. Behm, Phys. Rev. B **42**, 9307 (1990).
[12] D. D. Chambliss, R. J. Wilson, and S. Chiang, Phys. Rev. Lett. **66**, 1721 (1991).
[13] D. Fujita, T. Yakabe, H. Nejoh, T. Sato, and M. Iwatsuki, Surf. Sci. **366**, 93 (1996).
[14] B. Voigtländer, G. Meyer, and N. M. Amer, Phys. Rev. B **44**, 10 345 (1991).
[15] U. Harten, A. M. Lahee, J. P. Toennies, and Ch. Wöll, Phys. Rev. Lett. **54**, 2619 (1985).
[16] M. El-Batanouny, S. Burdick, K. M. Martini, and P. Stancioff, Phys. Rev. Lett. **58**, 2762 (1987).
[17] S. Narasimhan and D. Vanderbilt, Phys. Rev. Lett. **69**, 1564 (1992).
[18] L. C. Davis, M. P. Everson, R. C. Jaklevic, and W. Shen, Phys. Rev. B **43**, 3821 (1991).
[19] J. Tersoff and D. R. Hamann, Phys. Rev. B **31**, 805 (1985).
[20] J. E. Ortega, F. J. Himpsel, R. Haight, and D. R. Peale, Phys. Rev. B **49**, 13 859 (1994).
[21] E. Bertel, Surf. Sci. **331–333**, 1136 (1995).